Dog hepatocytes are key effector cells in the liver innate immune response to *Leishmania infantum*

Author for correspondence: Gabriela
M. Santos-Gomes, E-mail: santosgomes@ihmt.unl.pt

A. Rodrigues[1], G. Alexandre-Pires[2], A. Valério-Bolas[1], D. Santos-Mateus[1],
M. Rafael-Fernandes[1], M. A. Pereira[1], D. Ligeiro[3], T. Nunes[4], R. Alves-Azevedo[1],
S. Lopes-Ventura[1], M. Santos[2], A. M. Tomás[5], I. Pereira da Fonseca[2]
and G. Santos-Gomes[1]

[1]Global Health and Tropical Medicine, GHTM, Instituto de Higiene e Medicina Tropical, IHMT, Universidade Nova de Lisboa, UNL, Rua da Junqueira 100, 1349-008 Lisboa, Portugal; [2]CIISA, Centre for Interdisciplinary Research in Animal Health, Faculty of Veterinary Medicine, University of Lisbon, Av. Universidade Técnica, 1300-477 Lisbon, Portugal; [3]IPST-Centro de Sangue e Transplantação de Lisboa, Alameda das Linhas de Torres 117, 1749-005 Lisbon, Portugal; [4]Microscopy Center, Faculty of Sciences, Campo Grande, 1749-016 Lisbon, Portugal and [5]I3S, Instituto de Investigação e Inovação em Saúde, IBMC, Instituto de Biologia Molecular e Celular and, Instituto de Ciências Biomédicas Abel Salazar, ICBAS Universidade do Porto, Rua Alfredo Allen 208, 4200-135 Porto, Portugal

Abstract

Hepatocytes constitute the majority of hepatic cells, and play a key role in controlling systemic innate immunity, *via* pattern-recognition receptors (PRRs) and by synthesizing complement and acute phase proteins. *Leishmania infantum*, a protozoan parasite that causes human and canine leishmaniasis, infects liver by establishing inside the Kupffer cells. The current study proposes the elucidation of the immune response generated by dog hepatocytes when exposed to *L. infantum*. Additionally, the impact of adding leishmanicidal compound, meglumine antimoniate (MgA), to parasite-exposed hepatocytes was also addressed. *L. infantum* presents a high tropism to hepatocytes, establishing strong membrane interactions. The possibility of *L. infantum* internalization by hepatocytes was raised, but not confirmed. Hepatocytes were able to recognize parasite presence, inducing PRRs [nucleotide oligomerization domain (NOD)1, NOD2 and Toll-like receptor (TLR)2] gene expression and generating a mix pro- and anti-inflammatory cytokine response. Reduction of cytochrome P 450s enzyme activity was also observed concomitant with the inflammatory response. Addition of MgA increased NOD2, TLR4 and interleukin 10 gene expression, indicating an immunomodulatory role for MgA. Hepatocytes seem to have a major role in coordinating liver's innate immune response against *L. infantum* infection, activating inflammatory mechanisms, but always balancing the inflammatory response in order to avoid cell damage.

Introduction

The liver performs a remarkable number of life-supporting functions that influence all physiologic systems. The main essential functions of the liver are related to protein synthesis and metabolism, including amino acids, carbohydrate, lipid and vitamin metabolism. Also, the degradation of toxins, xenobiotics and waste products are essential functions performed by the liver (Mitra and Metcalf, 2009). *Leishmania infantum*, a protozoan parasite, and the agent of zoonotic visceral leishmaniasis (ZVL) and canine leishmaniasis (CanL) is able to target the liver, establishing inside the Kupffer cells (KC), the liver resident macrophages (Kaye and Beattie, 2016). Although not considered a lymphoid organ, the liver is also responsible for several immune functions, such as the removal of pathogens and exogenous antigens from the systemic circulation and production of several immune components. Hepatocytes constitute the majority of the hepatic cells and, although their primary role is of metabolic nature, they also play a key role in controlling systemic innate immunity *via* pattern-recognition receptors (PRRs) and trough production of complement plasma components (Szabo *et al.*, 2006; Sarma and Ward, 2011; Jenne and Kubes, 2013). These elements of the innate immune system represent an evolutionarily conserved first line of defense against pathogens. During an acute phase or a systemic inflammatory response, a variety of pro-inflammatory cytokines, such as interleukin (IL)-6, IL-1, tumour necrosis factor (TNF)-α and interferon (IFN)-γ can stimulate hepatocytes to produce high levels of complement and secreted PRRs (Gao *et al.*, 2007). The liver, not only is the major source of secreted PRRs, but also expresses membrane-bound PRRs, such as Toll-like receptors (TLRs) and intracellular PRRs such as nucleotide oligomerization domain (NOD)-like receptors, that recognize pathogen-associated molecular patterns (PAMPs). Hepatocytes express innate immune receptors and in many cases, have been demonstrated that recognize pathogen-associated ligands and display an innate immune response (Zhou *et al.*, 2016). TLRs play a vital role in viral and parasitic infections of the liver, in ischaemia-reperfusion injury, and in toxic liver damage, promoting antipathogen immunity but also hepatocellular injury and fibrogenesis (Bigorgne and Crispe, 2010; Broering

et al., 2011). Hepatocytes express messenger RNAs for all known TLRs, but their role in hepatocyte defense against invading pathogens is less clear. NODs comprise another family of intracellular PRRs, that are important for recognition of cell damage and of PAMPs. NOD1 and NOD2 are specialized NOD-like receptors that participate in the recognition of a subset of pathogenic microorganisms that are able to invade and multiply intracellularly (Franchi *et al.*, 2009; Scott *et al.*, 2010). Once activated, these receptors trigger intracellular signalling pathways that lead to the activation of transcriptional responses, culminating in the expression of a subset of inflammatory genes. NODs role is not yet well defined in liver immunology (Inohara and Nuñez, 2001; Scott *et al.*, 2010). In the context of CanL, the role of TLRs and NODs is still poorly understood. In humans, dogs and in genetically susceptible mice, the liver, the spleen and the bone marrow are major sites for the growth of visceral *Leishmania* parasites and development of associated pathology. Although there is some evidence regarding the immune response of target organs against *Leishmania* parasites from murine models (Stanley and Engwerda, 2007; Bankoti and Stäger, 2012), less is known about the specific immune responses occurring in these organs in humans and dogs (Sanchez *et al.*, 2004; Alexandre-Pires *et al.*, 2010; Rodríguez-Cortés *et al.*, 2016). One remarkable aspect of murine visceral leishmaniasis (VL) is the distinct growth rate of parasites in infected organs. Infection in the liver is characterized by a rapid increase in the parasite burden, followed by clearance of the parasite (Murray, 2008). This self-curing mechanism in the liver is attributed to the development of a T helper (Th)1 granulomatous response characterized by a high production of IFN-γ by CD4$^+$ T cells. Indeed, granulomas are poorly formed in sick dogs and patients with progressive VL, that do not develop mature granulomas. Livers of asymptomatic dogs showed an effective immunity with well-organized granulomas able to isolate and restrain parasite spreading, in an immune environment of activated effector T cells, dendritic cells (DCs) and central memory cells. In contrast, liver of symptomatic dogs showed a non-organized and ineffective infiltrate of T cells and heavily parasitized KCs (Sant'Ana *et al.*, 2007; Murray, 2008). Despite these local responses, *Leishmania* is able to disseminate and produce symptomatic VL. The parasite is able to target and alter the function of the host immune system by suppressing host protective Th1 responses, generate defective CD8$^+$ T cells and inhibit DC function (Ato *et al.*, 2006). Interacting with different cell subsets and inducing IL-10 production, the parasite generates an immunosuppressive environment, thus favouring its survival in the host (Smelt *et al.*, 2000; Olivier *et al.*, 2005; Gupta *et al.*, 2013). Curiously, the role played by hepatocytes in orchestrating the immune response and/or in the granuloma formation in the context of a *L. infantum* infection has not yet been addressed. As hepatocytes constitute the majority of the hepatic cells and in recent years have been shown that hepatocytes play a key role in innate immunity, we aimed to elucidate the innate immune response exhibited by hepatocytes in the presence of *L. infantum* parasites, by assessing the impact on cell metabolism and immune response. The effect of meglumine antimoniate (MgA), as a leishmanicidal compound, in the immune response produced by hepatocytes was also explored.

Methods

Leishmania infantum *parasites*

Leishmania infantum zymodeme MON-1 (MHOM/PT/89/IMT151) were cultured in Schneider's drosophila medium with L-glutamine (SCHN, Sigma-Aldrich) supplemented with 10% (v/v) of heat-inactivated foetal bovine serum (FBS, Sigma-Aldrich) and penicillin–streptomycin (Biochrom) at 100 U ml^{-1} and 100 μg ml^{-1} respectively (complete SCHN medium) at 24 °C. Only virulent parasites with less than five passages were used (Santos-Gomes and Abranches, 1996). To differentiate *L. infantum* axenic amastigotes, stationary phase virulent promastigotes (2×10^6 parasites ml^{-1}) were inoculated into complete SCHN medium (pH 5.5) supplemented with 2% of filtered human urine (from a healthy male donor). Cultures were incubated at 37 °C under a humidified atmosphere with 5% CO_2 for 3 weeks to allow complete amastigote transformation. Amastigote differentiation was followed by inverted microscopy (Olympus, CKX41) and confirmed with a scanning electronic microscope (JEOL5200-LV). Green fluorescent protein (GFP)-expressing *L. infantum* promastigotes (Marques *et al.*, 2015) were maintained in culture, using complete SCHN medium supplemented with 25 μg ml^{-1} of geneticin (Sigma-Aldrich). GFP-amastigotes were also obtained using the complete SCHN medium above described supplemented with 25 μg ml^{-1} of geneticin. Amastigote differentiation was confirmed under a fluorescence microscope equipped with a GFP filter (Nikon eclipse 80i) and Nikon DS-Ri1 camera.

Hepatocyte isolation

Hepatocyte cells were isolated from 12 livers of healthy dogs (*Canis lupus familiaris*), by an adapted two-step perfusion protocol followed by collagenase digestion and a Percoll® gradient centrifugation (Miranda *et al.*, 2009, 2010). A hepatic lobe was cleaned externally with a NaCl solution supplemented with 0.9% of penicillin/streptomycin and blood perfusion was performed with Perfusion I solution [2.4 M ethylene glycol tetraacetic acid, 142 mM NaCl, 6.7 mM KCl and 10 mM 4-(2-hydroxyethyl)-1-piperazineethanesulphonic acid (HEPES) at pH 7.4] heated at 38 °C. To digest tissue collagen, allowing the release of single hepatocytes, a second perfusion was implemented using the Perfusion II solution (67 mM NaCl, 6.7 mM KCl, 100 mM HEPES, 4.8 mM CaCl$_2$, pH 7.6) supplemented with 250 mg of collagenase H (Roche) and 0.5% albumin (Prolabo®), heated at 38 °C. The cell suspension was filtered through sterile gauze and centrifuged at 50 g for 10 min at 4 °C. Pellets were re-suspended in Williams' E medium (Sigma-Aldrich) and 3.5×10^6 cells ml^{-1} resuspended in 6 ml of Williams' E medium were overlaid into 20 ml of 25% Percoll® (GE Healthcare) in 1× phosphate-buffered saline (PBS) and centrifuged at 1300 g for 20 min at 4 °C. Viable hepatocytes were washed two times with cold 1× PBS and the final pellet was resuspended in supplement Williams' E medium [penicillin (100 U ml^{-1})/streptomycin (100 μg ml^{-1}) (Sigma-Aldrich), 1.4 μM hydrocortisone (Sigma-Aldrich), 15 mM HEPES (Sigma-Aldrich), 1 mM sodium pyruvate (Sigma-Aldrich), 1 mM non-essential amino acids (Biochrom), 40 μg ml^{-1} gentamycin (Sigma-Aldrich) and 10% (v/v) FBS]. Cells (5×10^5 cells ml^{-1}) were plated in a 24 well-plate and medium replaced with fresh medium at 24, 48 and 72 h post-isolation. During all procedures, cells were routinely followed by an inverted microscope and digital images were acquired with an Olympus CS30 camera.

Hepatocyte exposure to L. infantum

L. infantum virulent promastigotes, axenic amastigotes, GFP-promastigotes or GFP-axenic amastigotes were washed with PBS, added to hepatocytes in a proportion of 3:1 parasites per hepatocyte and left to incubate for 72 h at 37 °C under a humidified atmosphere with 5% CO_2. Samples of medium and cells were collected from duplicate wells at 1.5, 3, 5, 24, 48 and 72 h. Non-exposed control hepatocytes were also incubated for 72 h. As a positive control of inflammation, *Escherichia coli* lipopolysaccharide (LPS, Sigma-Aldrich) was added to hepatocyte cultures

($1 \mu g\ ml^{-1}$) and incubated for 72 h. Cultures were followed by optical microscopy observation under an inverted microscope and digital images were acquired.

Meglumine antimoniate

After 72 h of incubation, fresh medium and $100\ \mu M$ of MgA ($300\ mg\ Sb^V\ ml^{-1}$, Glucantime®-Merial) was added to hepatocytes (control) and to hepatocytes exposed to *L. infantum* amastigotes, ensuring the minimal cell disturbance. Cells were incubated at 37 °C under a humidified atmosphere with 5% CO_2. Samples of medium and cells were collected from duplicate wells at 1.5, 3, 5, 24, 48 and 72 h of incubation with MgA. Cultures were followed by optical microscopy observation under an inverted microscope.

Parasite viability

To estimate the viability of parasites (*L. infantum* amastigotes) that were in contact with hepatocytes in the presence of MgA, an adapted limit dilution assay (LDA) was performed. At each time point, the culture medium was removed, causing minimal disturbance to adherent hepatocytes and parasites, and sediments were re-suspended in 1 ml of complete SCH medium. Cell suspension ($200\ \mu l$) was added to the first column wells of a sterile 96 well plate and 1:4 serial dilutions were done. Plates were sealed and incubated at 24 °C for 15 days. In parallel, amastigote-to-promastigote differentiation in the absence of hepatocytes or MgA was used as a control. Samples were collected in duplicate and LDA performed in quadruplicate. Each well was observed under an inverted optical microscope and the presence of motile promastigotes was registered as positive titres. Parasite viability was estimated by the rate between the reciprocal of the obtained titres and the reciprocal of the highest positive titres obtained for amastigote differentiation without previous contact with hepatocytes or drug (control).

Hepatocyte viability

To ensure that hepatocytes were viable during MgA treatment, the mitochondria's reducing ability was evaluated using resazurin (7-hydroxy-3H-phenoxazin-3-one-10-oxide – Sigma-Aldrich). At each time point, $25\ \mu l$ of a 1.25 mM resazurin solution in $1\times$ PBS was added to each well and incubated for 24 h. Plates were read in a fluorometer (TRIADTM 1065, DYNEX Technologies) with excitation and emission wavelengths of 535 and 595 nm, respectively. Non-treated hepatocytes (viable cells) and paraformaldehyde (Sigma-Aldrich) fixed hepatocytes (non-viable cells) were used as controls.

Assessment of cell–parasite interrelation

The interplay of parasites with hepatocytes was observed by fluorescent microscopy and scanning electron microscopy (SEM). Hepatocytes (2.5×10^5 cells ml^{-1}) were cultured for 72 h in an eight-well chamber slides with cover (Lab-Tek II, Nunc) at 37 °C under a humidified atmosphere with 5% CO_2. *L. infantum* GFP-amastigotes or GFP-promastigotes were added to cultured cells in a proportion of three parasites per cell. Cells were incubated with the parasite for 1.5, 3, 5, 24, 48 and 72 h. Adherent cells were washed with $1\times$ PBS and fixed with PBS 2% paraformaldehyde (m/v) for 20 min on ice. Cells were then permeabilized with PBS 1% Tween-20 (v/v) (Sigma-Aldrich) and 0.2% fish gelatin (m/v) (Sigma-Aldrich) overnight at 4 °C and then incubated in PBS 1% Tween-20 (v/v) 0.125% fish gelatin (m/v) with anti-actin goat polyclonal antibody fluorescein isothiocyanate

conjugated (sc-1616, Santa Cruz) (1:500) and anti-ferritin goat polyclonal antibody (sc-14416, Santa Cruz) (1:100) for 90 min at room temperature. These polyclonal antibodies are described as having cross-reactivity with several species, including the dog. For the anti-ferritin staining, a rabbit anti-goat immunoglobulin-G secondary polyclonal antibody-Alexa Fluor® 647 (ab150143, Abcam) was used at a dilution of 1:500. Between primary and secondary antibodies, cells were washed three times with PBS 0.08% Tween-20 (v/v) and finishing by three more washes with $1\times$ PBS. Slides for fluorescence microscopy were stained with TO-PRO®-3 that has a red-fluorescent compound and digital images were acquired in a Leica TCS SP2 Laser Scanning Confocal Microscope. For SEM hepatocytes were washed with cold $1\times$ PBS and fixed with 2% paraformaldehyde (m/v) in PBS for 20 min on ice. Cells were washed again with cold $1\times$ PBS by centrifugation at 350 ***g*** for 10 min, filtrated through a Millipore mesh and subsequently dehydrated in a graded ethanol series [30, 50, 70, 80, 90 and 100% (v/v)]. Samples were dried using the critical point drying method, coated with gold palladium and mounted on stubs. Cells were then observed in a scanning electronic microscope (JEOL5200-LV) and digital images were acquired.

Real-time polymerase chain reaction analysis

To evaluate the immune response exhibited by hepatocytes, gene expression of cell sensors and cytokines were quantified by a real-time polymerase chain reaction (PCR) quantitative method, using previous described primers (Rodrigues *et al.*, 2017). RNA extraction was performed using a NZY Total RNA Isolation kit (Nzytech Genes & Enzymes) and cDNA synthesis was done with a NZY First-strand cDNA Synthesis kit (Nzytech Genes & Enzymes) according to the manufacturer's indications. Real-time PCR was performed in a 7500 FAST Real-Time PCR System thermal cycler (Applied Biosystems). Amplification was carried out as described in Rodrigues *et al.* (2017). External cDNA standards were constructed for all target genes by cloning PCR fragments, generated by the same primers, into a pGEM®-TEasy Vector according to the manufacturer's recommendations (Promega, USA) and as described by Rodrigues *et al.* (2006). The number of copies of each gene was normalized to the housekeeping gene β-actin, in order to regularize differences in relative quantities of initial cDNA in the sample. The final results for each gene were expressed as the log of the number of gene copies per 1000 copies of β-actin.

Urea and nitric oxide production

Urea and nitrate/nitrite quantification was performed using a commercial kit QuantiChrom™ Urea Assay Kit-DIUR-500 (BioAssay System) and Nitrate/Nitrite Colorimetric Assay kit (Abnova) respectively, accordingly with the manufacturer's recommendations. For urea quantification, the intensity of the colour, measured at 450 nm, is proportional to the urea concentration in the sample. Supernatants of cell cultures were centrifuged at 500 ***g*** for 10 min and plated ($50\ \mu l$ well^{-1}) in a 96 well plate (Nunc). Standard urea concentration and blank (water) were included and calculations were performed accordingly to the manufacturer's instructions. For nitrate/nitrite quantification, a standard curve was obtained with nitrate 1:5 serial dilutions and blank (medium) and supernatants of cell cultures centrifuged at 500 ***g*** for 10 min were plated ($80\ \mu l$ per well) in a 96 well plate. Absorbance was measured at 550 nm (BioRad-680, microplate reader). Supplement hepatocyte culture medium Williams' E was also assessed and its value reduced to all samples, to avoid any interference.
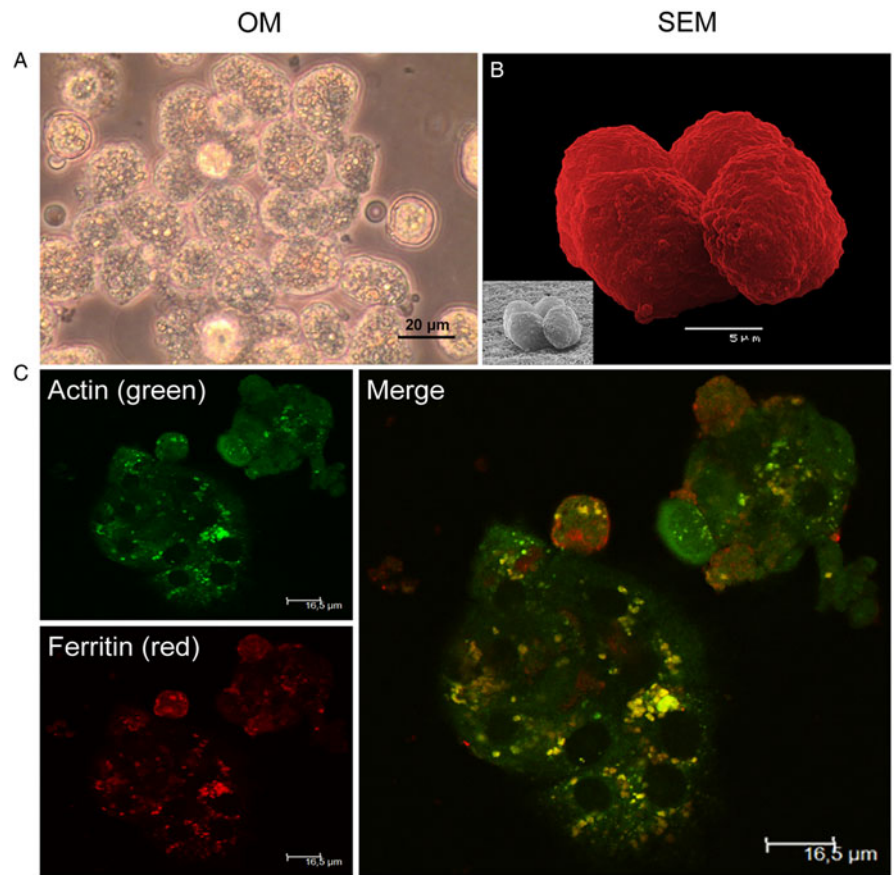
OM   SEM

Fig. 1. Hepatocyte morphology. Cell samples with 24 (A) and 48 h (B) of culture were observed under an optical inverted microscope (A, scale bar: 20 *μm*, ×400 magnification) and a SEM (B) and images were acquired. Individualized cells with round shape, nucleus and abundance of intracellular organelles (A) with a tendency to aggregate (A, B and C) were identified. Hepatocytes with a smooth cell membrane were observed 48 h after isolation (B). Artificial colour (B) was applied to cells (red) to evidence cell morphology. Hepatocytes incubated for 72 h (C) were stained for actin (green), a component of cell cytoskeleton, and for ferritin (red), usually prevailing in secretory vesicles. Cells were observed under a fluorescence confocal microscope and images were acquired. The characteristic rounded shape of individualized hepatocytes, nuclei (black round spots) and cell aggregates are also observed.

Cytochrome P (CYP) 450s enzyme activity

Activity of phase I alkoxyresorufin O-dealkylation (AROD) of CYP450 family in hepatocytes exposed to parasites and MgA was analysed using the following substrates: 7-ethoxyresorufin (EROD, dog CYP1A1 and CYP1A2 enzymes), 7-methoxyresorufin (MROD, dog CYP1A2 and CYP1B), 7-pentoxyresorufin (PROD, dog CYP2B11) or 7 benzyloxyresorufin (BROD, dog CYP2B11, CYP3A12 and CYP3A26). All substrates were purchased from Sigma-Aldrich and dissolved in Williams' E medium with 10 μM dimethyl sulphoxide. After careful removal of the medium, fresh culture medium containing 10 μl of substrates was added to hepatocytes and left to incubate for 1 h at 37 °C under a humidified atmosphere with 5% CO_2. Then, supernatants were collected in duplicate and centrifuged to eliminate any debris. In a sterile 96 well black plate (Nunc), 200 μl of each sample was plated in triplicate. A standard curve was performed with resorufin (Sigma-Aldrich) and the fluorescence was read on a fluorometer with excitation and emission wavelengths of 535 and 595 nm, respectively. As for phase II uridine 5′-diphospho-glucuronosyltransferase (UDP-glucuronosyltransferase, UGT), cells were incubated with fresh culture medium with a final concentration of 10 mM of 4-methylumbelliferone (4-MU) (Sigma-Aldrich), during 1 h at 37 °C under a humidified atmosphere with 5% CO_2. The assay was performed in duplicate. After incubation, supernatants were centrifuged at 500 *g*, for 10 min at 4 °C and analysed in triplicate by fluorescence emission on a fluorometer (BIOTEK® FLx800) with excitation at 360/40 nm and emission at 460/40 nm. A standard curve was performed with 4-MU, starting at 10 mM and followed by 1:2 serial dilutions. 4-MU mobilization was calculated by subtracting the amount detected in samples to the initial amount of 4-MU. A blank constituted by Williams' E culture medium, a substrate control assay and, culture medium was also included.

Statistical analysis

The non-parametric Wilcoxon test for two related samples was used to compare differences between time points and different experimental conditions. Data analysis was performed using software IBM SPSS Statistics version 16.0 (IBM, USA). A significance level of 5% ($P < 0.05$) was used as indicative of statistical significance.

Results

Hepatocytes interact with L. infantum *parasites*

Cells isolated from dog livers presented typical hepatocyte morphology, exhibiting a round shape, prominent nucleus and abundant intracellular organelles associated with metabolic and secretory functions, easily observed due to refrangibility of light (Fig. 1A). Cell membrane topography evidenced a smooth aspect (Fig. 1B), indicating the absence of major perturbations caused by the isolation process. Furthermore, hepatocytes showed a network of actin microfilaments in the cytoskeleton (Fig. 1C) and several spots of actin deposition (green spots), probably indicating secretory vesicles. Cells also exhibited spots staining for ferritin (red), some of which co-localized with actin. The presence of high levels of ferritin, a complex that stores and releases iron in a controlled way, has been described as characteristic of these cells.

To investigate how hepatocytes sense and respond to the presence of *L. infantum*, plated hepatocytes were exposed to amastigote and promastigote morphological forms. Parasites evidenced a strong tropism for hepatocytes, directly interacting with the cell membrane (Figs 2 and 3), indicating that *L. infantum* is highly attracted by hepatocytes. In some cases, parasites even seemed to be uptake by hepatocytes (Fig. 3, 24 h incubation) but in a non-conclusive way. After 5 h of parasite exposure
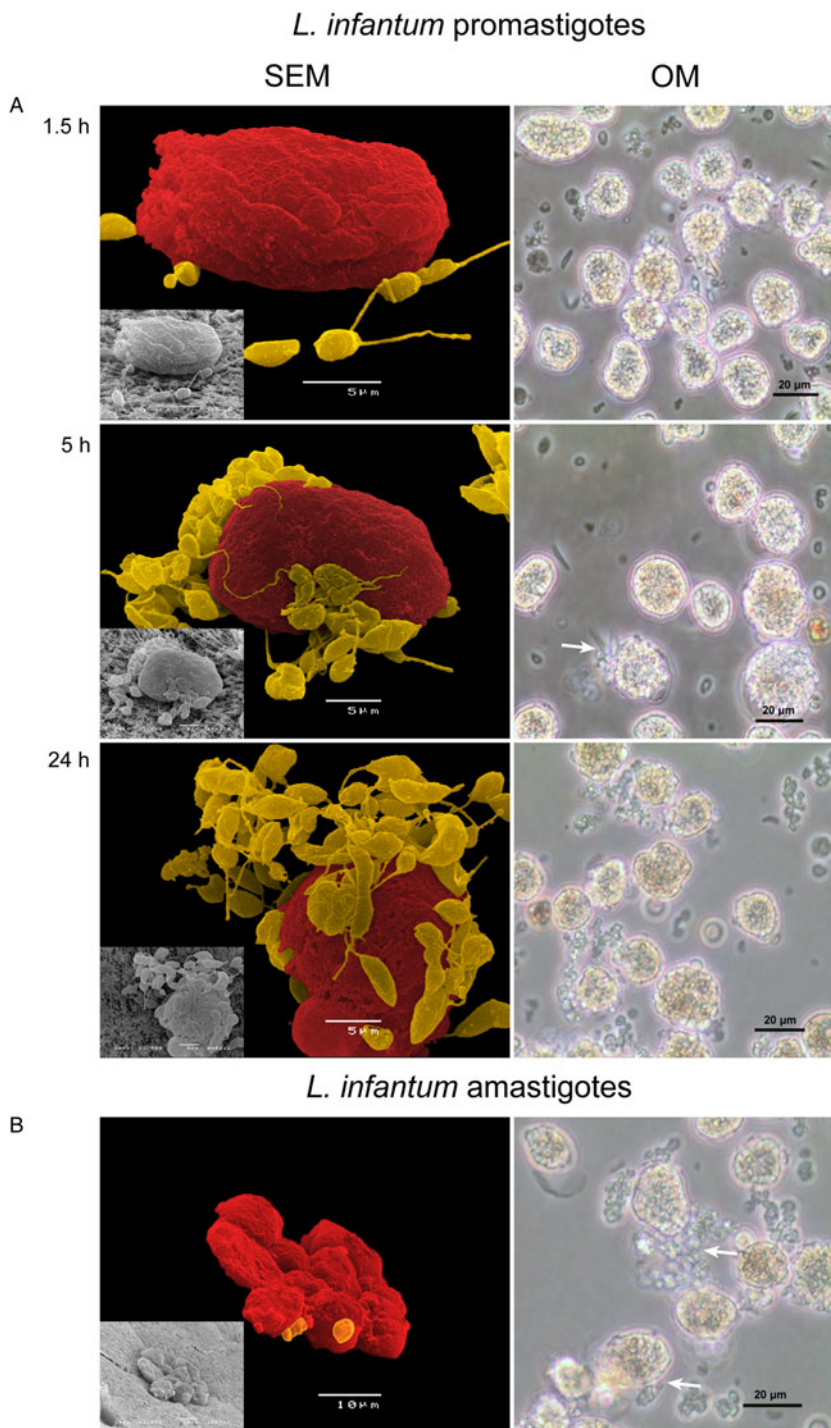
Fig. 2. Hepatocytes exposed to *L. infantum*. (A) Culture samples obtained at 1.5, 5 and 24 h of promastigotes exposure were collected and observed under an inverted microscope (OM, scale bar: 20 μm, ×400 magnification) and a SEM and images were acquired. At early parasite exposure (1.5 h), promastigotes are in the proximity of hepatocytes but, with incubation time, promastigotes surround the hepatocyte (5 h) and parasite interaction with the cell membrane of hepatocyte becomes evident (24 h). The interaction of the parasite with the cell membrane (white arrows) can be observed. SEM images artificial coloured evidenced the close interaction of the promastigote form (yellow) and the hepatocyte membrane (red). Culture samples obtained at 24 h of amastigotes exposure were collected and observed under an inverted microscope (OM, scale bar: 20 μm, ×400 magnification) and SEM and images were acquired (B). The interaction of the parasite with the cell membrane (white arrows) can be seen and parasites exhibiting amastigote morphological characteristics can be observed. SEM images artificial coloured evidenced the close interaction of the amastigote form (yellow) and the hepatocyte membrane (red).

(Figs 2A and 3), parasites appeared to be strongly attached to hepatocyte membrane, remaining linked over the 72 h of incubation. Promastigote flagella were observed in close connection to the hepatocyte membrane (Fig. 2, 5 and 24 h of incubation), while the amastigote membrane was bound to hepatocyte cell membrane (Fig. 2B). In addition, promastigotes seemed to induce hepatocytes to generate more vesicles rich in actin filaments, what is probably related to increased secretion (Fig. 3). After 5 h of promastigote exposure, ferritin spots were enlarged and localized, mainly in the cell membrane region, pointing towards the sequestration of ferritin (Fig. 3, 5 and 24 h of incubation).

Hepatocyte metabolism is disturbed by *L. infantum* parasites

In order to better characterize the hepatocyte response to *L. infantum*, several metabolic parameters were assessed. Urea constitutes a hepatocyte characteristic detoxification product and is highly influenced by the presence of inflammatory stimuli. Accordingly, while hepatocytes non-exposed to *L. infantum* presented a steady urea production, when in contact (1.5 h) with amastigotes ($P = 0.0313$) or promastigotes ($P = 0.0156$), they reacted with a burst of urea production (Fig. 4A), similarly to what is observed upon LPS stimulation ($P = 0.0313$) which was used here as a positive control. This suggests that parasites are sensed by hepatocytes as a cause of stress. After 24 h of exposure to parasites, hepatocytes reduced the urea production significantly ($P_{\text{amastigotes}} = 0.0313$, $P_{\text{promastigotes}} = 0.0156$). *De novo* urea production decreased to minimal values after 72 h of parasite exposure and LPS-stimulation ($P_{\text{amastigotes, promastigotes, LPS}} = 0.0313$). Hepatocytes non-exposed to *L. infantum* evidenced a residual nitric oxide (NO) and the exposure to parasites increased NO production (Fig. 4B). The levels of NO in cells incubated
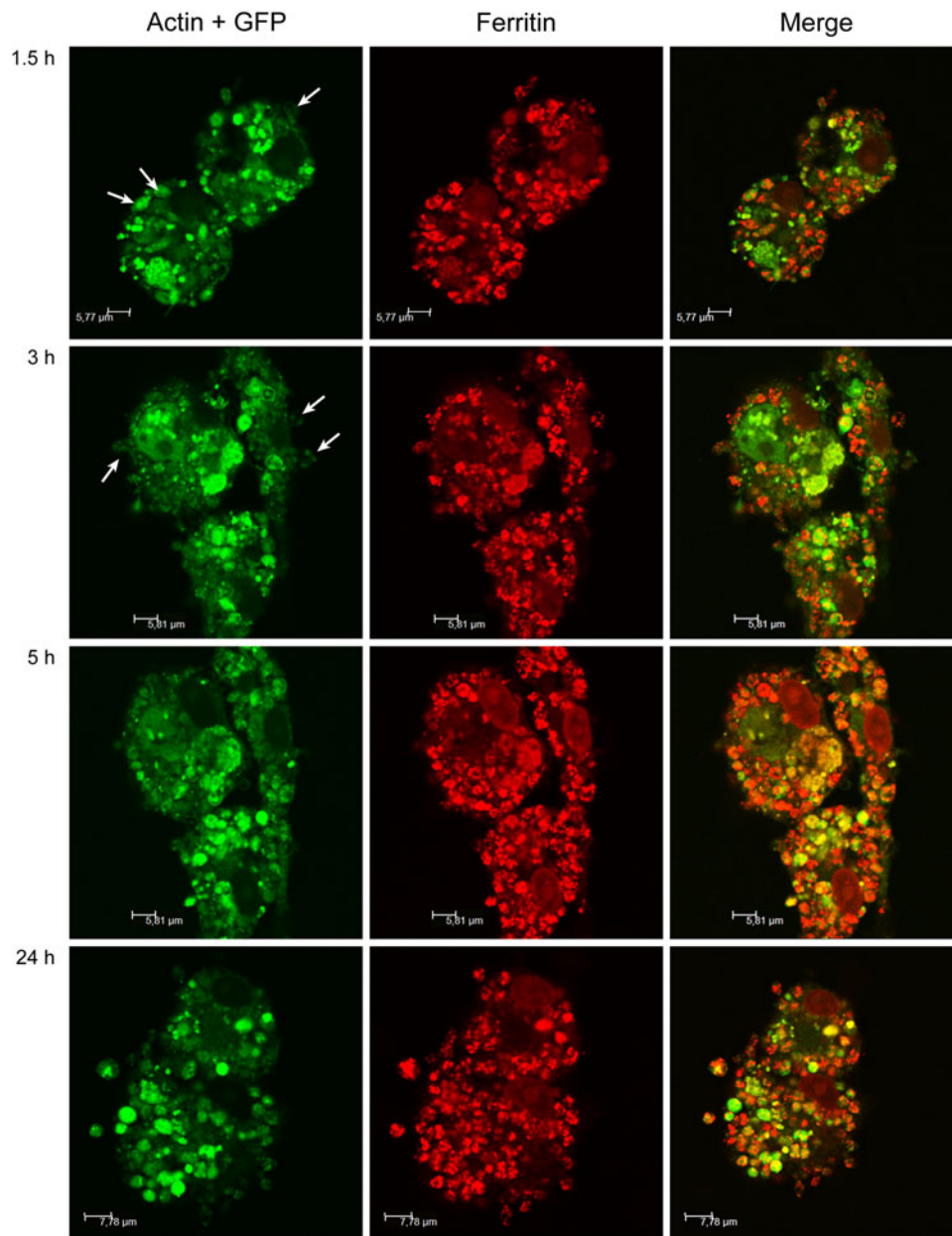
Fig. 3. Actin and ferritin in cultured hepatocyte exposed to *L. infantum* virulent promastigotes. Hepatocytes incubated for 24 h in the presence of *L. infantum* promastigotes (with arrows) were stained for actin (green), a component of cell cytoskeleton, and for ferritin (red), frequently present in secretory vesicles. Cells were observed under a fluorescence confocal microscope and images were acquired. Hepatocytes present a large round nucleus (stained red by TO-PRO®). Promastigotes exhibit a high tropism to hepatocytes and seem to induce hepatocyte to generate more vesicles (5 h).
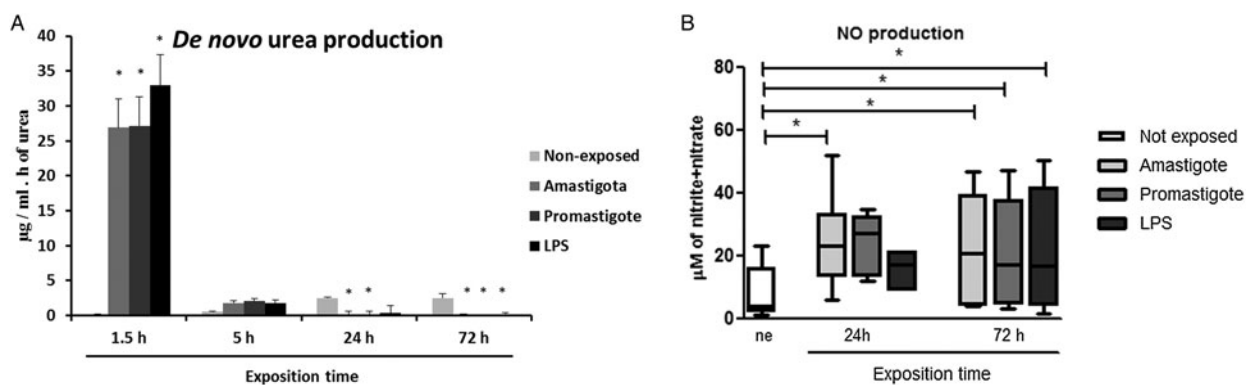

Fig. 4. Production of urea and NO by hepatocytes exposed to *L. infantum*. Hepatocytes were used to evaluate *de novo* production of urea (A) and NO (B) after 72 h of exposure to amastigotes or promastigotes. In parallel, non-exposed hepatocytes and LPS-stimulated hepatocytes were also evaluated as negative and positive controls, respectively. Results of samples of 12 livers performed in triplicate are represented by mean and standard error (A) or by box plots and whiskers (median, minimum to maximum) (B). The non-parametric Wilcoxon test was used for statistical comparisons. *Represents values of statistical significance ($P < 0.05$) when comparing non-exposed hepatocytes *vs* the other conditions.
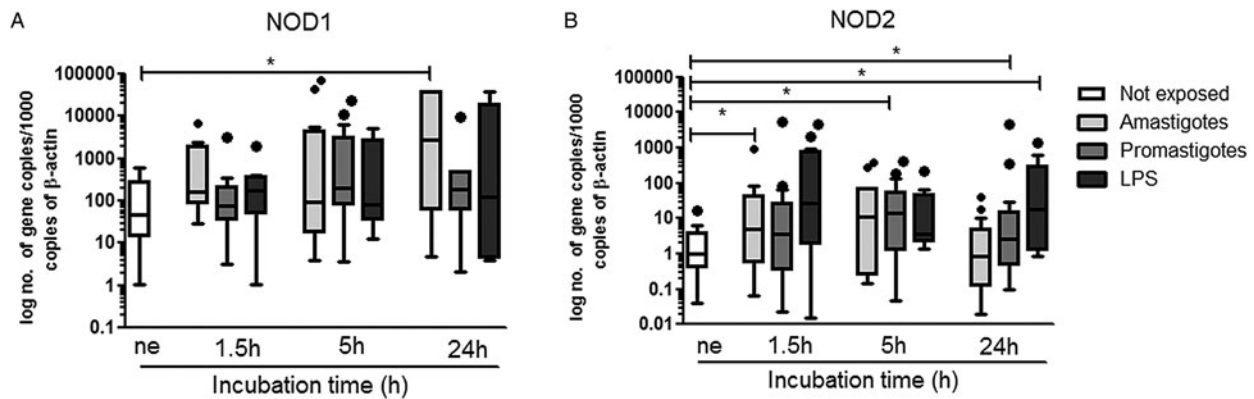
Fig. 5. (A) NOD1 and (B) NOD2 gene expression in hepatocytes exposed to *L. infantum.* Hepatocytes were used to evaluate NOD1 and NOD2 mRNA accumulation for 24 h of exposure to amastigotes or promastigotes. Hepatocytes not exposed to parasites and LPS-stimulated hepatocytes were also evaluated. Results of samples of 12 liver performed in triplicate are represented by Tukey graphs. Black dots are indicative of outlier values. The non-parametric Wilcoxon test was used for statistical comparisons ($P < 0.05$). *Represents values of statistical significance when comparing not-exposed hepatocytes *vs* the other conditions.

with parasites for 24 h were significantly higher than those of non-stimulated cells. High NO levels were sustained for 72 h in the presence of amastigotes ($P = 0.0313$) and promastigotes ($P = 0.0469$), as well as of LPS stimulated cells ($P = 0.0469$).

CYP450 enzymes, commonly designated as phase I enzymes and phase II UGT enzyme were assessed to investigate how inflammatory stimuli might influence hepatocyte xenobiotic metabolism (Supplementary Fig. 1). Results indicate that *L. infantum* presence, regardless of the parasite morphological form used, tends to slight disturb the normal activity of CYP450 enzymes.

Hepatocytes sense and react to L. infantum parasites

The early immune response triggered by hepatocytes exposed to *L. infantum* amastigotes or promastigotes was assessed by evaluating the gene expression of innate immune receptors (TLR2, TLR4, TLR9, NOD1 and NOD2) and of cytokines (IL-10, TNF-α and IL-6) by real-time PCR. Compared with resting hepatocytes, amastigotes progressively induced the increase of NOD1 gene expression that reached significant values after 24 h ($P = 0.0371$) (Fig. 5A). Hepatocytes exposed to amastigotes also exhibited an increase of NOD2 mRNA (Fig. 5B) at 1.5 h ($P = 0.0195$). Promastigote exposure led to the increase of NOD2 mRNA at 5 h ($P = 0.0020$) and 24 h ($P = 0.0353$) when compared with resting cells. These responses are in line with those triggered by the positive control that induced a significant increase of NOD2 gene expression ($P = 0.0049$) upon 24 h of exposure. Gene expression of TLR2, TLR4 and TLR9 showed some fluctuation although not significantly different from resting hepatocytes.

Taken together, these findings suggest that hepatocyte immune status is disturbed by both *L. infantum* morphological forms, generating intracellular NOD1 and NOD2. The observed fluctuations of TLR mRNA seem to reflect a probable hepatic tolerance to parasites as no major expression increase was observed (Supplementary Fig. 2).

An initial and transitory burst of IL-10 mRNA was detected in hepatocytes exposed to amastigotes ($P = 0.0269$, Fig. 6A) while promastigotes generated a notorious augment of IL-10 after 24 h ($P = 0.0186$). LPS-stimulated hepatocytes also reacted with an increase in IL-10 mRNA at 1.5 h ($P = 0.0024$) and at 5 h ($P = 0.0049$). Gene expression of pro-inflammatory IL-6 was low throughout the study (Fig. 6B), except at 5 h of hepatocyte contact with promastigotes where an increase of IL-6 mRNA was found ($P = 0.0342$). When compared with resting hepatocytes, gene expression of pro-inflammatory TNF-α increased significantly in hepatocytes exposed to promastigotes from 1.5 to 5 h

($P_{1.5 \text{ h}} = 0.0391$, $P_{5 \text{ h}} = 0.0389$) (Fig. 6C). However, long (24 h) exposure to amastigotes was needed for hepatocytes to exhibit a significant accumulation of TNF-α mRNA ($P = 0.0245$). LPS-stimulated hepatocytes presented a steady increase of TNF-α mRNA ($P_{1.5 \text{ h}} = 0.0186$, $P_{5 \text{ h}} = 0.0210$) over the first 5 h of incubation.

These results indicate that the contact with *L. infantum* induces hepatocytes to generate pro- and anti-inflammatory cytokines.

Treatment with MgA stimulates both immunity and metabolism of hepatocytes exposed to L. infantum parasites

To verify the viability of hepatocytes in the presence of MgA, a resazurin assay was performed. The assay demonstrated that addition of MgA to cultured hepatocytes did not disturb cell viability throughout the 72 h of incubation (Fig. 7A). The leishmanicidal potential of MgA in the presence of hepatocytes plus *L. infantum* was evaluated through an adapted limiting dilution assay (Fig. 7B). As expected, MgA exhibited a strong leishmanicidal activity that increased with the time of contact. At 1.5 and 5 h incubation, a significant inhibition of parasite viability was obtained ($P_{1.5 \text{ h}} = 0.0355$; $P_{5 \text{ h}} = 0.0271$) when compared with non-treated parasites. After 24 h of treatment, the inhibition of parasite growth reached the 100% and no viable parasites were observed. Also, the activity of phase I (EROD, BROD, MROD and PROD assays) and phase II (UGT assay) enzymes were assessed in the presence of MgA. All the phase I enzymes evaluated showed an increased activity rate in the presence of MgA (Fig. 8). The addition of MgA to amastigote-exposed hepatocytes induced the significant augment of EROD ($P_{1.5, 24, 72 \text{ h}} = 0.0156$; $P_{5 \text{ h}} = 0.0313$) (Fig. 8A), BROD ($P_{1.5-72 \text{ h}} = 0.0156$) (Fig. 8B), MROD ($P_{1.5-72 \text{ h}} = 0.0313$) (Fig. 8C) and PROD ($P_{5, 24, 72 \text{ h}} = 0.0313$) (Fig. 8D) activities throughout the time points evaluated when compared with untreated amastigote-exposed hepatocytes. Curiously, phase II UGT showed a steady activity profile over the observation time (Fig. 8E).

These results reflect an important increase in CYP450 activities, indicating that MgA might be metabolized by CYP1A1, CYP1A2, CYP2B11, CYP3A12, CYP3A26 and CYP1B enzymes.

After treatment, NOD1 gene expression of hepatocytes exposed to amastigotes remained similar to non-treated amastigote-exposed hepatocytes (Fig. 9A). On the contrary, the addition of MgA to amastigote-exposed hepatocytes for 5 h led to an increase of NOD2 mRNA ($P = 0.0162$, Fig. 9A). TLR gene expression remained similar to non-treated amastigote-exposed hepatocytes
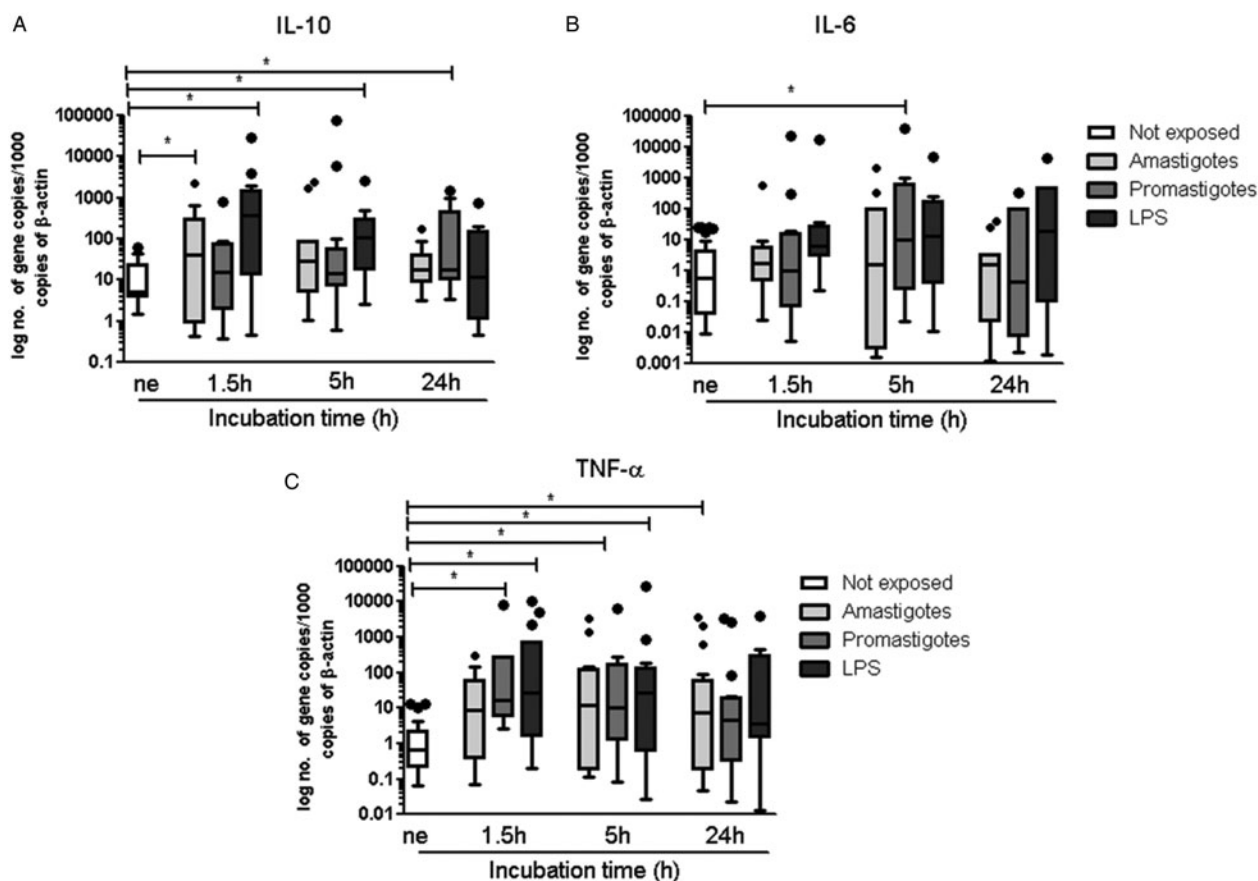
Fig. 6. Gene expression of IL-10, IL-6 and TNF-α by hepatocytes exposed to *L. infantum*. Hepatocytes were used to evaluate IL-10 (A), IL-6 (B) and TNF-α (C) mRNA accumulation for 24 h of exposure to amastigotes or promastigotes. Non-exposed hepatocytes and LPS-stimulated hepatocytes were also evaluated. Results of samples of 12 livers performed in triplicate are represented by Tukey graphs. Black dots are indicative of outlier values. The non-parametric Wilcoxon test was used for statistical comparisons ($P < 0.05$). *Represents values of statistical significance when comparing not-exposed hepatocyte *vs* the other conditions.
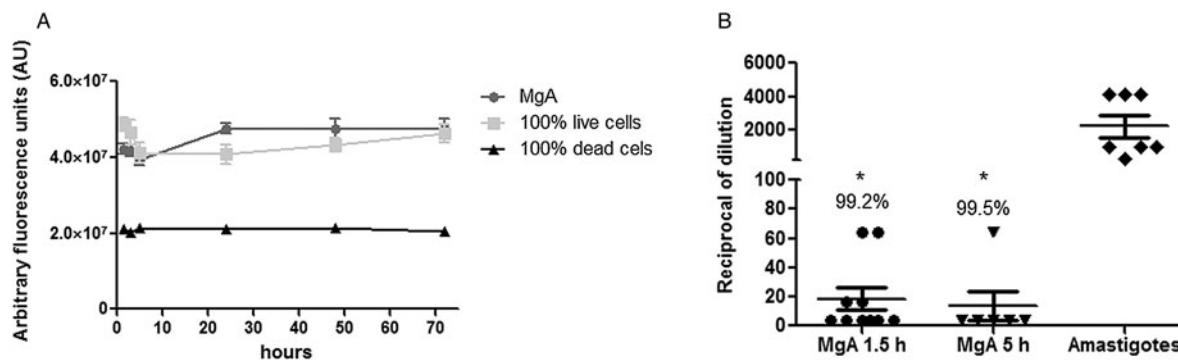

Fig. 7. Viability of dog hepatocytes and *L. infantum* axenic amastigotes exposed to MgA. The viability of 72 h-cultured hepatocytes incubated with MgA (A) was evaluated for more 72 h by a resazurin assay. Non-treated hepatocytes (living cells) and hepatocytes fixed with paraformaldehyde (dead cells) were evaluated in parallel. Samples of amastigote-exposed hepatocytes treated with MgA (B) for 1.5 and 5 h of incubation were plated in SCH medium and incubated at 24 ° C. In parallel, plated axenic amastigotes were also allowed to differentiate in promastigotes under the same conditions. The reciprocal of the last promastigote positive dilution was considered as indicative of viability. The non-parametric Wilcoxon test was used for statistical comparisons. *Indicates significant differences ($P < 0.05$). Inscribed values indicate the reduction obtained when compared to the amastigote reciprocal dilution (100% viability).

(Fig. 9B). TLR4 gene expression exhibited the unique exception, presenting a transient increase 5 h after MgA treatment ($P = 0.0049$) as a possible consequence of the high availability of parasite antigens, resulting from parasite death.

The addition of MgA to hepatocytes led to a transient change in the cytokine environment (Fig. 10). MgA significantly increased IL-10 gene expression ($P = 0.0098$) when compared with non-treated hepatocytes (Fig. 10A). However, IL-6 and TNF-α gene expression did not show important differences when compared with non-treated hepatocytes (Fig. 10B and C).

Altogether, these findings indicate that MgA induces canine hepatocytes to generate anti-inflammatory cytokine IL-10, probably to preserve immune homoeostasis, avoiding excessive inflammation.

Discussion

Hepatocytes constitute 70–85% of the liver's mass, undertaking vital roles in protein synthesis and storage, carbohydrate metabolism, cholesterol synthesis and detoxification by metabolization of
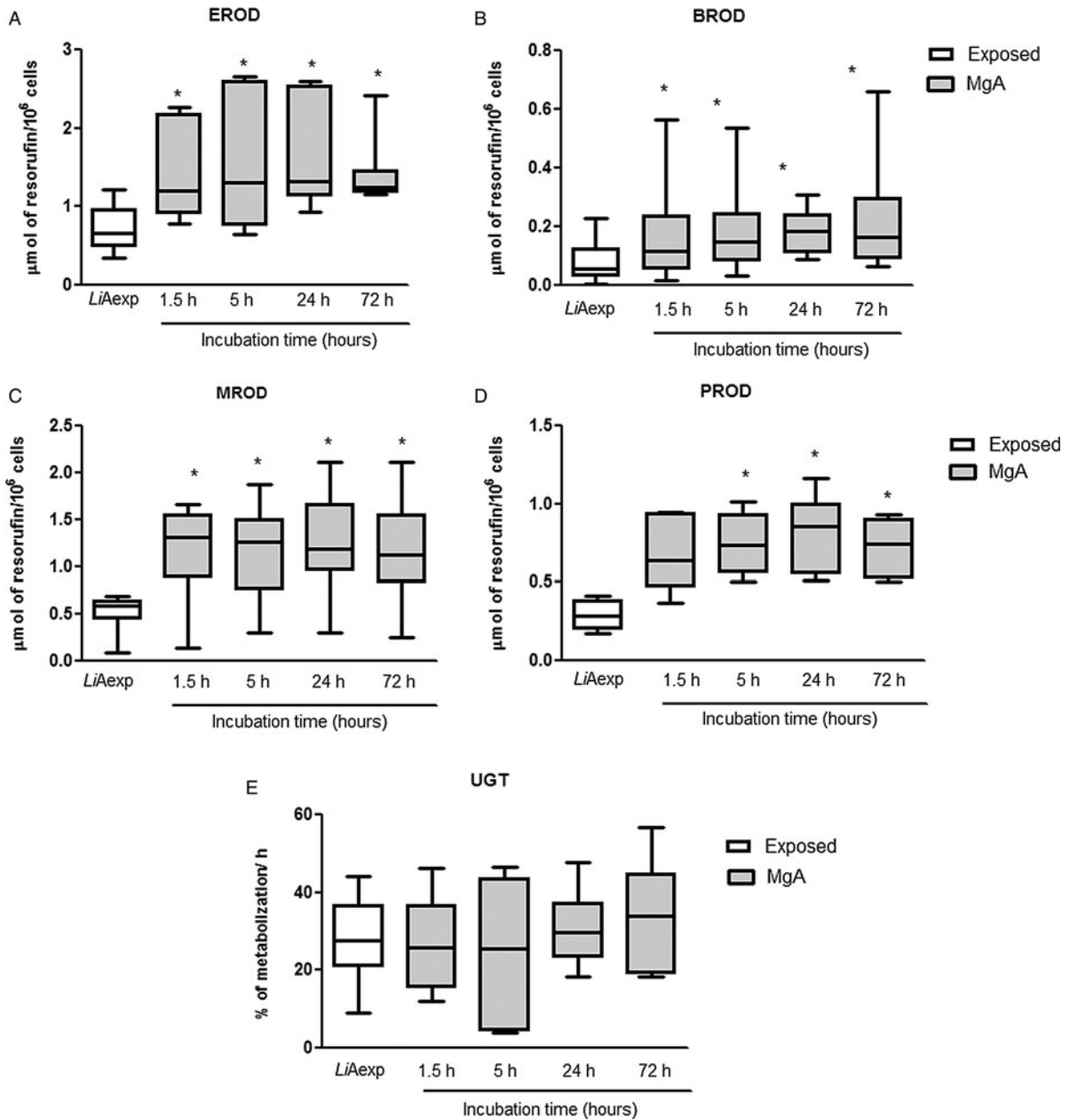
Fig. 8. Phase I and phase II enzyme activity after MgA treatment of hepatocytes exposed to *L. infantum* axenic amastigotes. Hepatocytes treated for 72 h were used to evaluate EROD (A), BROD (B), MROD (C), PROD (D) and UGT (E) enzyme activity. In parallel, the enzymatic activity of non-treated hepatocytes (*Li*Aexp) was also evaluated. Results of samples of 12 livers performed in triplicate are represented by box plots and whiskers (median, minimum to maximum). The non-parametric Wilcoxon test was used for statistical comparisons. *Represents statistical significance values ($P < 0.05$) when comparing non-treated amastigote-exposed hepatocytes *vs* treated amastigote-exposed hepatocytes.
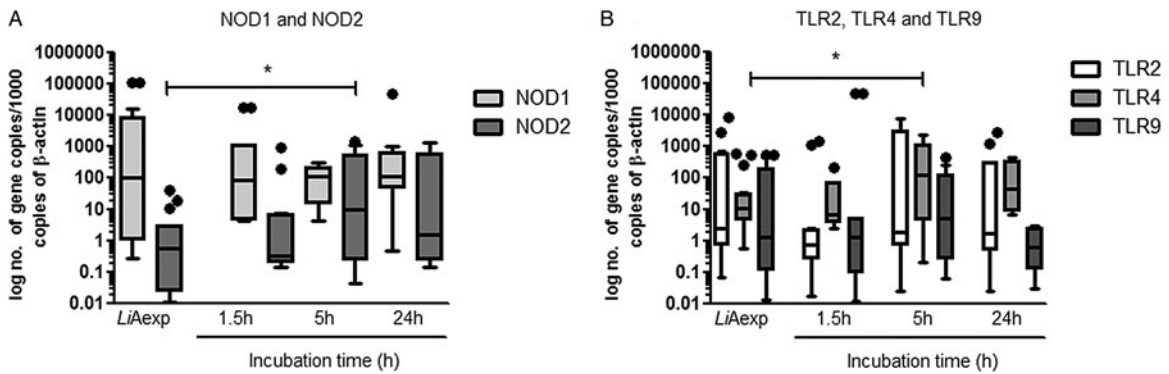

Fig. 9. Gene expression of PRRs by amastigote-exposed hepatocytes after MgA treatment. Hepatocytes treated with MgA were used to evaluate NOD1, NOD2 (A), TLR2, TLR4 and TLR9 (B) mRNA accumulation for 24 h. In parallel, PRR gene expression was also evaluated in non-treated amastigote-exposed hepatocytes (*Li*Aexp). Results of samples of 12 livers performed in triplicate are represented by Tukey graphs. Black dots are indicative of outlier values. The non-parametric Wilcoxon test was used for statistical comparisons. *Indicates statistically important differences ($P < 0.05$) when comparing treated and non-treated hepatocytes.
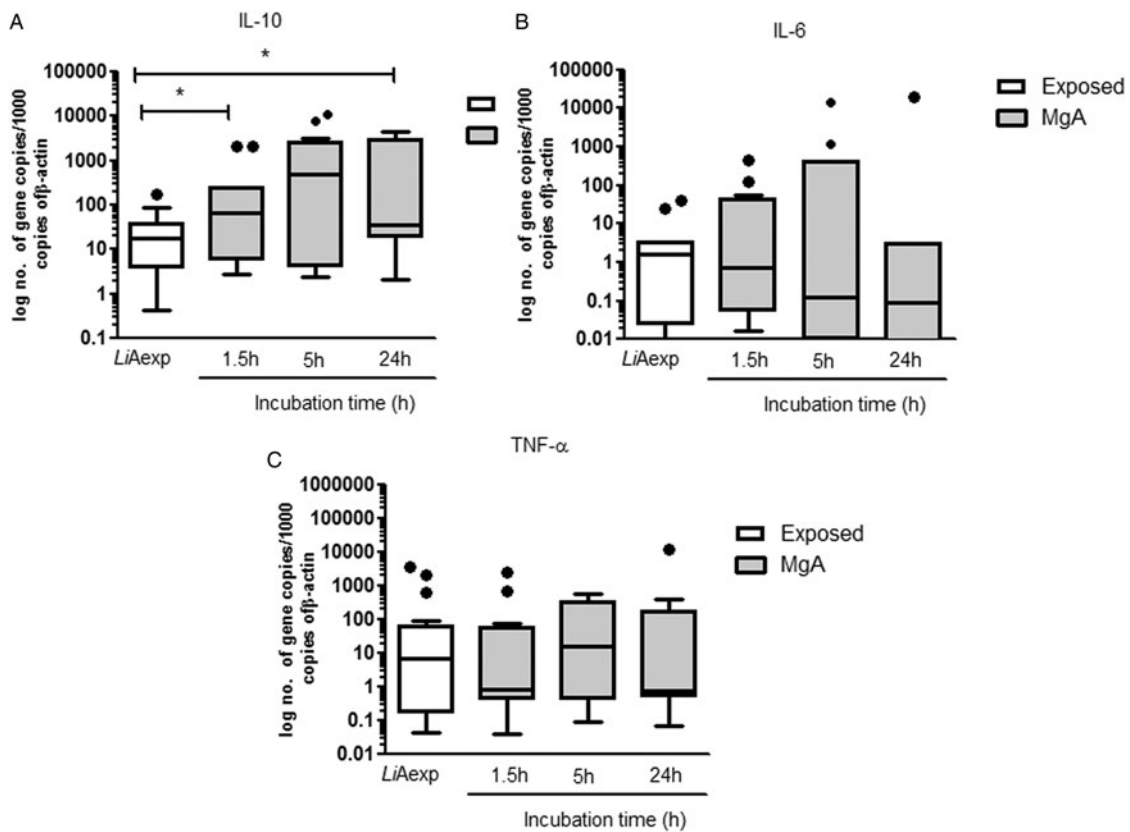
Fig. 10. Gene expression of IL-10, IL-6 and TNF-α by hepatocytes exposed to *L. infantum* axenic amastigotes after MgA treatment. Hepatocytes treated with MgA for 24 h and non-treated amastigote-exposed hepatocytes (*Li*Aexp) were used to evaluate IL-10, (A), IL-6 (B) and TNF-α (C) mRNA accumulation. Results of samples of 12 livers performed in triplicate are represented by Tukey graphs. Black dots are indicative of outlier values. The non-parametric Wilcoxon test was used for statistical comparisons. *Represents statistical significance values ($P < 0.05$) when comparing non-treated *vs* treated hepatocytes.

exogenous and endogenous substances. Adding to these traditional hepatocyte associated functions, in recent years it has been revealed that hepatocytes also play essential roles in immune homoeostasis by controlling systemic innate immunity *via* production of secreted PRRs and of complement components found in plasma.

The liver is a main target organ of *L. infantum*. In contrast to the spleen that stays chronically infected, infection in the liver is normally self-containing. Resolution of disease in this organ is associated with granuloma formation, which is one of the key features of hepatic resistance. The resolution of the infection in the liver (in humans, dogs and mouse models) is attributed to the development of a Th1-dominated granulomatous response, that is able to restrain the parasite dissemination and is characterized by high IFN-γ, IL-12 and TNF-α production through CD4^{+} T cells (Sant'Ana *et al.*, 2007; Melo *et al.*, 2009; Kaye and Beattie, 2016). IL-12 has been described, as an essential cytokine in the development of protective immunity against *Leishmania*. Blocking this cytokine reduces both IFN-γ production and granuloma formation in the liver of infected mice (Murray *et al.*, 2006). Hepatic resistance is attributed to the generation of reactive nitrogen and oxygen intermediates, both of which have been shown to play a role in containing parasite growth during the early stages of infection (Murray and Nathan, 1999; Mahmoud *et al.*, 2016). Hepatocytes express membrane-bound PRRs, such as TLRs and NODs that can be triggered by exogenous ligands derived from pathogens or by endogenous ligands resulting from cellular injury, activating the immune response. TLR and NOD recognition is often associated with the production of pro-inflammatory cytokines and generation of effector molecules, which promote differentiation of Th1 cells, leading to an inflammatory response (Murray and Nathan, 1999; Mahmoud *et al.*, 2016). In the current

work, the gene expression of NOD1 and NOD2, as well as TLR2, TLR4 and TLR9 exhibited by hepatocytes after exposure to *L. infantum* was assessed. Amastigote and promastigote exposure seems to be able to trigger hepatocyte immune response by inducing NOD2 gene expression, while increases in NOD1 gene expression seem to be caused only by the amastigote form and after a long time of parasite exposure. It is possible that the increased gene expression of these intracellular PRRs leads to the activation of inflammatory and protective immune response against *L. infantum* parasites, which is reflected by increased NO production and TNF-α generation. However, only a few *Leishmania*-derived molecules have been reported to activate PRRs, being the most described the surface lipophosphoglycan (Becker *et al.*, 2003). Thus, the potential role played by the innate immune receptors of hepatocytes in surveillance and activation against *L. infantum* parasites is not easy to clarify. The current work constitutes the first report addressing the innate immune response exhibited by canine hepatocytes in the presence of *L. infantum*. As the majority of studies were performed in MØ, it makes it difficult a direct comparison with hepatocytes. MØ constitutes the final host cells for *Leishmania*, but the parasite or parasite antigenic fractions may establish a direct contact with other non-immune cells, such as hepatocytes, which can sense and react to them, influencing the immune response outcome. The close interaction of parasites with hepatocyte's membrane together with the generation of intracellular PRRs NOD1 and NOD2 raised the hypothesis that *L. infantum* might be internalized by canine hepatocytes. Hepatocytes are known to display phagocytic activity under special circumstances, although not in a uniform manner (Soji *et al.*, 1992; Dini *et al.*, 2002). There is evidence for the presence of *L. donovani* amastigotes within hepatocytes in liver biopsies from VL patients having undergone

through successful therapy (Duarte *et al.*, 1989). Gangneux *et al.* (2005) demonstrated *in vitro* that murine, rat and human primary hepatocytes were permissive to *L. donovani* promastigote infection, but parasites did not massively proliferate. Nevertheless, these findings bring into question a possible role for hepatocytes as a parasite reservoir, during host latent infection. The current study gives evidence that hepatocytes can be permissive to both morphological forms of *L. infantum*. Parasites exhibited a clear tropism to hepatocytes and the interaction with the hepatocyte membrane seems to be very strong. Furthermore, parasites can induce gene expression of internal PRRs, raising the question of a possible synergistic effect of both NOD1 and NOD2 in leading to the activation of hepatocytes to produce inflammatory cytokines IL-6 and TNF-α and breaking the immune tolerance that characterizes the liver tissue, initiating a protective immune response. These findings indicate that hepatocytes are active cells in innate immune surveillance and that are able to initiate an immune response.

Leishmania species are known to trigger MØ phagocytosis by establishing ligation with surface receptors on these cells, facilitating *Leishmania* internalization. These include the first and third complement receptor (CR1 and CR3, respectively), mannose receptor, Fc gamma receptors (FcγRs, in particular FcγRII-B2) and fibronectin receptors (FnRs) (Ueno and Wilson, 2012), that act in synchrony with CR to phagocyte pathogens. It is described the presence of FnRs (Johansson *et al.*, 1987) and Fc receptors in adult hepatocytes (Blumberg *et al.*, 1995). By itself FnRs may retain the pathogen, possibly being the major responsible for the close interaction of *L. infantum* parasites with the hepatocyte membrane unravelled in this study.

During the present experimental procedure, hepatocytes were viable and metabolically active, positive for ferritin, a non-toxic form of iron storage and transport and presenting urea production, which is a characteristic of functional hepatocytes. Furthermore, hepatocytes reacted to the presence of LPS, generating TNF-α and IL-10. Hepatocyte culture, although not representing the full complexity of the liver, constitutes an effective tool for understanding how hepatocytes can be activated and orchestrate an immune response, and how they react to pathogens.

Hepatocytes also sense and react to *L. infantum* parasites, generating immunomediators. IL-6 is a pleiotropic cytokine with beneficial effects in the liver. This cytokine promotes liver regeneration and protects against a multitude of liver-damaging factors. IL-6 together with TNF-α and IL-1 is required for induction of the acute phase response, which has been regarded as part of an attempt to maintain homoeostasis, promoting microorganism opsonization and activating complement, or neutralizing proteolytic enzymes (Streetz *et al.*, 2001; Gruys *et al.*, 2005). IL-6 has also been associated with some of VL characteristic clinical signs, such as fever. Downregulation of the hepatocytic acute phase receptors is achieved by rapid hepatic removal of circulating cytokines and release of IL-10, inducing tolerance and suppressing the local IL-6 production (Heinrich *et al.*, 1998; Jura and Koj, 2011). Exposure of hepatocytes to *L. infantum* parasites induced the expression of IL-10, together with IL-6 and TNF-α, probably in order to maintain hepatocyte homoeostasis, inducing tolerance and avoiding damages by excessive inflammation, which can have important negative consequences.

MgA is a classical leishmanicidal drug belonging to the pentavalent antimonial class. The addition of a leishmanicidal drug to hepatocytes exposed to parasites impacts the immune response, having a significant effect on cytokine generation and in the gene expression of innate immune receptors, not affecting hepatocyte viability. MgA treatment increased NOD2 and TLR4 gene expression and generated IL-10, suggesting amastigote killing and recognition of parasite release antigens by hepatocyte PRRs.

Furthermore, hepatocytes showed slight alteration in the CYPs activity when exposed to *L. infantum*, as a possible consequence of hepatocyte inflammation. Since the liver constitutes a major metabolic organ, impairment of liver functions may have a great impact on individual health. In humans and animals, infections or inflammatory stimuli can cause changes in the expression and activity of various forms of liver CYP450 (Morgan, 2009). However, the effects are not uniform for all CYPs, as they can be suppressed, unaffected or positively induced by inflammatory conditions. CYP1A1 and CYP1A2, CYP2B11, CYP1B, CYP3A12, and CYP3A26 were highly induced by the administration of MgA, indicating that this compound or a derived metabolite is metabolized by CYP450.

Hepatocytes constitute key cells in liver metabolism and also exhibit important immune functions with a vital role in VL. Hepatocytes were able to sense and react to *L. infantum* parasites, increasing PRR gene expression and generating pro-inflammatory cytokines. Furthermore, *L. infantum* parasites established a close interaction with hepatocyte membrane and induced expression of intracellular PRRs, raising the hypothesis that *L. infantum* might be internalized by dog hepatocytes, redefining the role of hepatocytes in CanL and, consequently questioning its importance in the epidemiology of ZVL. Altogether, these findings contribute to a better understanding of the liver as an innate immunological key organ.

Author ORCIDs. G. Santos-Gomes, 0000-0001-9264-3887.

References

Alexandre-Pires G, de Brito MT, Algueró C, Martins C, Rodrigues OR, Pereira da Fonseca I and Santos-Gomes G (2010) Canine leishmaniosis. Immunophenotypic profile of leukocytes in different compartments of symptomatic, asymptomatic and treated dogs. *Veterinary Immunology and Immunopathology* 137, 275–283.

Ato M, Maroof A, Zubairi S, Nakano H, Kakiuchi T and Kaye PM (2006) Loss of dendritic cell migration and impaired resistance to *Leishmania donovani* infection in mice deficient in CCL19 and CCL21. *Journal of Immunology* 176, 5486–5493.

Bankoti R and Stäger S (2012) Differential regulation of the immune response in the spleen and liver of mice infected with *Leishmania donovani*. *Journal of Tropical Medicine* 2012, 639304.

Becker I, Salaiza N, Aguirre M, Delgado J, Carrillo-Carrasco N, Kobeh LG, Ruiz A, Cervantes R, Torres AP, Cabrera N, González A, Maldonado C and Isibasi A (2003) *Leishmania* lipophosphoglycan (LPG) activates NK cells through toll-like receptor-2. *Molecular and Biochemical Parasitology* 130, 65–74.

Bigorgne AE and Crispe IN (2010) TLRs in hepatic cellular crosstalk. *Gastroenterology Research and Practice* 2010, 1–7.

Blumberg RS, Koss T, Story CM, Barisani D, Polischuk J, Lipin A, Pablo L, Green R and Simister NE (1995) A major histocompatibility complex class

I-related Fc receptor for IgG on rat hepatocytes. *The Journal of Clinical Investigation* **95**, 2397–2402.

Broering R, Lu M and Schlaak JF (2011) Role of toll-like receptors in liver health and disease. *Clinical Science* **121**, 415–426.

Dini L, Pagliara P and Carlà EC (2002) Phagocytosis of apoptotic cells by liver: a morphological study. *Microscopy Research and Technique* **57**, 530–540.

Duarte MIS, Mariano ON and Corbett CEP (1989) Liver parenchymal cell parasitism in human visceral leishmaniasis. *Virchows Archiv: A Pathological Anatomy and Histopathology* **415**, 1–6.

Franchi L, Warner N, Viani K and Nuñez G (2009) Function of NOD-like receptors in microbial recognition and host defense. *Immunological Reviews* **227**, 106–128.

Gangneux JP, Lemenand O, Reinhard Y, Guiguen C, Guguen-Guillouzo C and Gripon P (2005) *In vitro* and *ex vivo* permissivity of hepatocytes for *Leishmania donovani*. *Journal of Eukaryotic Microbiology* **52**, 489–491.

Gao B, Jeong WI and Tian Z (2007) Liver: an organ with predominant innate immunity. *Hepatology* **47**, 729–736.

Gruys E, Toussaint MJM, Niewold TA and Koopmans SJ (2005) Acute phase reaction and acute phase proteins. *Journal of Zhejiang University Science B* **6**, 1045–1056.

Gupta G, Oghumu S and Satoskar AR (2013) Mechanisms of immune evasion in leishmaniasis. *Advances in Applied Microbiology* **82**, 155–184.

Heinrich PC, Behrmann I, Muller-Newen G, Schaper F and Graeve L (1998) Interleukin-6-type cytokine signalling through the gp130/Jak/STAT pathway 1. *Biochemical Journal* **334**, 297–314.

Inohara N and Nuñez G (2001) The NOD: a signaling module that regulates apoptosis and host defense against pathogens. *Oncogene* **20**, 6473–6481.

Jenne CN and Kubes P (2013) Immune surveillance by the liver. *Nature Immunology* **14**, 996–1006.

Johansson S, Forsberg E and Lundgren B (1987) Comparison of fibronectin receptors from rat hepatocytes and fibroblasts. *The Journal of Biological Chemistry* **262**, 7819–7824.

Jura J and Koj A (2011) Regulatory mechanisms controlling inflammation and synthesis of acute phase proteins. In Veas F (ed.), *Acute Phase Proteins – Regulation and Functions of Acute Phase Proteins*. London, UK: IntechOpen Limited, pp. 61–84. ISBN: 978-953-307-252-4.

Kaye PM and Beattie L (2016) Lessons from other diseases: granulomatous inflammation in leishmaniasis. *Seminars in Immunopathology* **38**, 249–260.

Mahmoud AE, Attia RA, Eldeek HE, Farrag HMM and Makboul R (2016) Polymerase chain reaction detection and inducible nitric-oxide synthase expression of *Leishmania major* in mice inoculated by two different routes. *Tropical Parasitology* **6**, 42–50.

Marques CS, Passero LFD, Vale-Gato I, Rodrigues A, Rodrigues OR, Martins C, Correia I, Tomás AM, Alexandre-Pires G, Ferronha MH and Santos-Gomes GM (2015) New insights into neutrophil and *Leishmania infantum in vitro* immune interactions. *Comparative Immunology, Microbiology and Infectious Diseases* **40**, 19–29.

Melo FA, Moura EP, Ribeiro RR, Alves CF, Caliari MV, Tafuri WL, da Calabrese KS and Tafuri WL (2009) Hepatic extracellular matrix alterations in dogs naturally infected with *Leishmania* (*leishmania*) *chagasi*. *International Journal of Experimental Pathology* **90**, 538–548.

Miranda JP, Leite SB, Muller-Vieira U, Rodrigues A, Carrondo MJT and Alves PM (2009) Towards an extended functional hepatocyte *in vitro* culture. *Tissue Engineering Part C: Methods* **15**, 157–167.

Miranda JP, Rodrigues A, Tostões RM, Leite S, Zimmerman H, Carrondo MJT and Alves PM (2010) Extending hepatocyte functionality for drug-testing applications using high-viscosity alginate-encapsulated three-dimensional cultures in bioreactors. *Tissue Engineering Part C: Methods* **16**, 1223–1232.

Mitra V and Metcalf J (2009) Metabolic functions of the liver. *Anaesthesia & Intensive Care Medicine* **10**, 334–335.

Morgan ET (2009) Impact of infectious and inflammatory disease on cytochrome P450-mediated drug metabolism and pharmacokinetics. *Clinical Pharmacology and Therapeutics* **85**, 434–438.

Murray HW (2008) Tissue granuloma structure-function in experimental visceral leishmaniasis. *International Journal of Experimental Pathology* **82**, 249–267.

Murray HW and Nathan CF (1999) Macrophage microbicidal mechanisms *in vivo*: reactive nitrogen versus oxygen intermediates in the killing of intracellular visceral *Leishmania donovani*. *The Journal of Experimental Medicine* **189**, 741–746.

Murray HW, Tsai CW, Liu J and Ma X (2006) Responses to *Leishmania donovani* in mice deficient in interleukin-12 (IL-12), IL-12/IL-23, or IL-18. *Infection and Immunity* **74**, 4370–4374.

Olivier M, Gregory DJ and Forget G (2005) Subversion mechanisms by which *Leishmania* parasites can escape the host immune response: a signaling point of view. *Clinical Microbiology Reviews* **18**, 293–305.

Rodrigues OR, Moura RA, Gomes-Pereira S and Santos-Gomes GM (2006) H-2 complex influences cytokine gene expression in *Leishmania infantum*-infected macrophages. *Cellular Immunology* **243**, 118–126.

Rodrigues A, Santos-Mateus D, Alexandre-Pires G, Valério-Bolas A, Rafael-Fernandes M, Pereira MA, Ligeiro D, de Jesus J, Alves-Azevedo R, Lopes-Ventura S, Santos M, Tomás AM, Pereira da Fonseca I and Santos-Gomes G (2017) *Leishmania infantum* exerts immunomodulation in canine Kupffer cells reverted by meglumine antimoniate. *Comparative Immunology, Microbiology and Infectious Diseases* **55**, 42–52.

Rodríguez-Cortés A, Carrillo E, Martorell S, Todolí F, Ojeda A, Martínez-Flórez A, Urniza A, Moreno J and Alberola J (2016) Compartmentalized immune response in leishmaniasis: changing patterns throughout the disease. *PLoS ONE* **11**, 1–13.

Sanchez MA, Diaz NL, Zerpa O, Negron E, Convit J and Tapia FJ (2004) Organ-specific immunity in canine visceral leishmaniasis: analysis of symptomatic and asymptomatic dogs naturally infected with *Leishmania chagasi*. *The American Journal of Tropical Medicine and Hygiene* **70**, 618–624.

Sant'Ana JAP, Lima WG, Oliveira MR, Simões LA, Michalick MSM, Melo MN, Tafuri WL and Tafuri WL (2007) Hepatic granulomas in canine visceral leishmaniasis and clinical status. *Arquivo Brasileiro de Medicina Veterinária e Zootecnia* **59**, 1137–1144.

Santos-Gomes GM and Abranches P (1996) Comparative study of infectivity caused by promastigotes of *Leishmania infantum* MON-1, *L. infantum* MON-24 and *L. donovani* MON-18. *Folia Parasitologica* **43**, 7–12.

Sarma JV and Ward PA (2011) The complement system. *Cell and Tissue Research* **343**, 227–235.

Scott MJ, Chen C, Sun Q and Billiar TR (2010) Hepatocytes express functional NOD1 and NOD2 receptors: a role for NOD1 in hepatocyte CC and CXC chemokine production. *Journal of Hepatology* **53**, 693–701.

Smelt SC, Cotterell SE, Engwerda CR and Kaye PM (2000) B cell-deficient mice are highly resistant to *Leishmania donovani* infection, but develop neutrophil-mediated tissue pathology. *Journal of Immunology* **164**, 3681–3688.

Soji T, Murata Y, Ohira A, Nishizono H, Tanaka M and Herbert DC (1992) Evidence that hepatocytes can phagocytize exogenous substances. *The Anatomical Record* **233**, 543–546.

Stanley AC and Engwerda CR (2007) Balancing immunity and pathology in visceral leishmaniasis. *Immunology and Cell Biology* **85**, 138–147.

Streetz KL, Wüstefeld T, Klein C, Manns MP and Trautwein C (2001) Mediators of inflammation and acute phase response in the liver. *Cellular and Molecular Biology* **47**, 661–673.

Szabo G, Dolganiuc A and Mandrekar P (2006) Pattern recognition receptors: a contemporary view on liver diseases. *Hepatology* **44**, 287–298.

Ueno N and Wilson ME (2012) Receptor-mediated phagocytosis of *Leishmania*: implications for intracellular survival. *Trends in Parasitology* **28**, 335–344.

Zhou Z, Xu MJ and Gao B (2016) Hepatocytes: a key cell type for innate immunity. *Cellular & Molecular Immunology* **13**, 301–315.